Spectral analysis of the nonlinear relativistic Doppler shift in ultrahigh intensity Compton scattering

F. V. Hartemann, A. L. Troha, and N. C. Luhmann, Jr.
Department of Applied Science, University of California, Davis, California 95616

Z. Toffano
Ecole Supérieure d'Electricité, 91192 Gif-sur-Yvette, France

(Received 17 April 1996)

The relativistic dynamics of an electron subjected to the classical electromagnetic field of an ultrashort laser pulse is studied theoretically at arbitrary intensities. Frequency modulation effects associated with the nonlinear relativistic Doppler shift induced on the backscattered radiation are analyzed in detail. For circular polarization, an exact analytical expression for the full nonlinear spectrum is derived. For linear polarization, it is found that the scattering of coherent light by a single electron describing a well-behaved trajectory can yield anharmonic spectra when the laser ponderomotive force strongly modulates the electron's proper time. At ultrahigh intensities, these nonlinear relativistic spectra exhibit complex structures. In addition, the temporal laser pulse shapes best suited to generate narrow Compton backscattered spectral lines at ultrahigh intensities are discussed. [S1063-651X(96)02009-0]

PACS number(s): 42.65.−k, 42.50.Lc, 41.60.−m, 42.50.Vk

I. INTRODUCTION

The recent advent of extremely high power, ultrafast lasers using fiber compression [1], Kerr-lens mode locking [2], and chirped pulse amplification (CPA) [3–5] makes it possible to study Compton scattering experimentally at ultrahigh intensities, where the normalized vector potential associated with the laser wave exceeds unity. For a wavelength of 1 μm, this translates into a focused intensity larger than 0.055 TW/μm^2. In this regime, the ponderomotive force acting on an electron colliding with the laser pulse can induce a strong axial velocity modulation, which, in turn, results in a nonlinear relativistic Doppler shift on the radiation backscattered by the electron during the interaction. This phenomenon can be analyzed in terms of frequency modulation. This type of effect, as well as ponderomotive scattering [6] and radiation damping [7–10], are expected to play an important role in the physics of the proposed γ-γ collider. Although the quantum electrodynamical nature of the electron-photon interaction must be taken into account for a full description of such phenomena, it is hoped that a large class of interactions may be appropriately studied within the context of high field strength classical electrodynamics. In addition, a thorough understanding of that topic is required for a comprehensive approach to high field QED. Finally, the framework of classical electrodynamics should be approximately valid for an intense laser when the number of photons scattered by the electron is sufficiently high and the coherence of the laser allows the indefinite number of photons to be treated as a classical, continuous electromagnetic field.

In this paper we consider ultrahigh intensity Compton scattering and first demonstrate that the spectrum of the forward-scattered wave is always identical to that of the pump field. We then analyze the spectrum of the backscattered wave and show how the nonlinear Doppler shift induced by the radiation pressure of a laser pulse on the electron during the interaction results in strong frequency modulation effects, yielding relativistic nonlinear spectra. This analysis is done within the framework of classical electrodynamics, which should remain appropriate as long as the average number of photons scattered by the electron is high, thus allowing the photon field to be treated as a classical, continuous electromagnetic field. The spectral properties of the scattered light and their behavior under Lorentz transformation are examined in detail. In the case of circular polarization, an analytical expression of the nonlinear backscattered spectrum is derived. To our knowledge, this represents the first exact derivation of the full nonlinear spectrum in ultrahigh intensity Compton backscattering.

This derivation indicates that at very high laser intensities, nonlinear spectra are obtained, where the scattered light is distributed over a large number of lines, even in the case of circularly polarized light. To alleviate this problem, holographic filtering techniques [11] can be used at the Fourier plane of the chirped pulse laser amplifier and are planned to be fully described within the context of ultrahigh intensity Compton scattering applications in a future paper. In the present work, we indicate what temporal laser pulse shapes are best suited to generate narrow Compton backscattered spectral lines, without covering the technical details of their implementation on a CPA laser.

We consider the motion of a relativistic electron submitted to the electromagnetic field of an ultrashort laser pulse propagating *in vacuo*. Diffraction effects are neglected, as well as radiative corrections [7–10]. This second approximation is valid as long as the laser wavelength, as measured in the instantaneous rest frame of the electron, is much longer than the classical electron radius ($a=2.8178\times10^{-15}$ m); this condition is satisfied in most experimental situations, except for ultrarelativistic electron beams, such as the Stanford Linear Accelerator Center (SLAC) beam, where the laser field can also approach the Schwinger critical field. At this point, it is important to note that in order to provide a correct interpretation of the nonlinear Compton scattering experiments

currently under way at SLAC [12], it is useful to take into account the effects studied in this paper as a zeroth-order classical description, which further motivates our approach.

This paper is organized as follows. In Sec. II we review the relativistic dynamics of a single electron subjected to the classical electromagnetic field of an intense, linearly or circularly polarized, ultrashort laser pulse in vacuum, neglecting radiative corrections (Lorentz-Maxwell electrodynamics) and diffraction. In Sec. III the spectral properties of the scattered light and their behavior under Lorentz transformation are examined. The nonlinear Doppler shift associated with the laser ponderomotive force is studied in Secs. IV and V. In the case of circular polarization (Sec. IV), an exact analytical expression for the full nonlinear spectrum is derived and we indicate what temporal laser pulse shapes are best suited to generate narrow Compton backscattered spectral lines. For linear polarization (Sec. V), it is shown that the scattering of coherent light by a single electron describing a well-behaved trajectory can yield anharmonic spectra when the laser ponderomotive force strongly modulates the electron's proper time and that these nonlinear relativistic spectra exhibit complex structures. Finally, conclusions are drawn in Sec. VI.

II. ELECTRON DYNAMICS AND CANONICAL INVARIANTS

The electron normalized four-velocity and four-momentum are defined as

$$u_\mu=\frac{1}{c}\frac{dx_\mu}{d\tau}=\gamma(1,\boldsymbol{\beta}),\quad p_\mu=m_0cu_\mu,$$

where τ is the proper time along the electron world line $x_\mu(\tau)$. The energy-momentum transfer equations are given by the Lorentz force

$$d_\tau u_\mu=-\frac{e}{m_0c}(\partial_\mu A_\nu-\partial_\nu A_\mu)u^\nu, \tag{1}$$

where we have introduced the four-vector potential of the laser wave

$$A_\mu=\left(\frac{\varphi}{c},\mathbf{A}\right),\quad \mathbf{A}=\hat{\mathbf{x}}A_x(\phi)+\hat{\mathbf{y}}A_y(\phi),\quad \varphi=0 \tag{2}$$

and defined the invariant phase of the traveling wave

$$\phi=\omega_0\left(t-\frac{z}{c}\right)=k^\mu x_\mu(\tau) \tag{3}$$

as a function of the characteristic laser frequency ω_0. This form of the potential corresponds to a transverse plane wave propagating in vacuum.

Along the electron trajectory, we have the important relation

$$d_\tau\phi=\omega_0(\gamma-u_z). \tag{4}$$

The energy-momentum transfer equations now read

$$d_\tau u_{x,y}=\omega_0(\gamma-u_z)d_\phi a_{x,y}(\phi), \tag{5}$$

$$d_\tau u_z=d_\tau\gamma=\omega_0[u_x d_\phi a_x(\phi)+u_y d_\phi a_y(\phi)], \tag{6}$$

where $\mathbf{a}=e\mathbf{A}/m_0c$ is the invariant normalized vector potential of the laser wave. Equation (6) yields the well-known canonical momentum invariant [6]

$$\gamma-u_z=\gamma_0(1-\beta_0). \tag{7}$$

An important consequence of Eq. (7) is that the electron phase and proper time are proportional to within a constant: $d\phi/d\tau=\omega_0\gamma_0(1-\beta_0)$. Equation (5) can readily be integrated to obtain the transverse canonical invariants

$$u_{x,y}(\tau)=a_{x,y}(\phi). \tag{8}$$

Using the conservation of canonical momentum, the normalized electron energy and axial momentum are derived, with the result that

$$u_z(\tau)=\gamma_0\left[\beta_0+\mathbf{a}^2(\phi)\left(\frac{1+\beta_0}{2}\right)\right], \tag{9}$$

$$\gamma(\tau)=\gamma_0\left[1+\mathbf{a}^2(\phi)\left(\frac{1+\beta_0}{2}\right)\right]. \tag{10}$$

These results are quite general and hold as long as plane waves are considered [6]. An important difference between polarization states immediately appears: $\mathbf{a}^2(\phi)$ varies adiabatically as the pulse envelope for circular polarization, while there is an extra modulation at $2\omega_0$ for linear polarization. The transverse electron momentum depends linearly on the laser field, but the axial momentum modulation is a quadratic function of that field, as it results from the coupling of the transverse velocity to the laser magnetic field through the ponderomotive force. At low intensities, the radiation pressure of the laser pulse is negligible and the electron basically propagates through the laser pulse at constant axial velocity, while its transverse momentum is modulated at the Doppler-shifted laser frequency. This results in the radiation of the well-known free-electron laser (FEL) spectral lines on axis [13]. The situation is very different when the normalized vector potential of the laser wave exceeds unity: the strong modulation of the electron axial momentum results in a nonlinear Doppler shift that translates into frequency modulation effects.

III. SCATTERED LIGHT SPECTRA

To derive the spectrum of the scattered radiation, we shall need an expression of the electron's position as a function of its nonlinear phase ϕ. We change variables

$$d_\phi\mathbf{x}=\frac{d_t\mathbf{x}}{d_t\phi}=\frac{c\boldsymbol{\beta}}{\omega_0(1-\beta_z)}=\frac{c\gamma\boldsymbol{\beta}}{\omega_0\gamma(1-\beta_z)}=\frac{c\mathbf{u}}{\omega_0\gamma_0(1-\beta_0)}. \tag{11}$$

Equation (9) can be formally integrated to obtain the electron's axial position

$$z(\phi)=\frac{c}{\omega_0(1-\beta_0)}\int_{-\infty}^{\phi}\left[\beta_0+\mathbf{a}^2(\psi)\left(\frac{1+\beta_0}{2}\right)\right]d\psi. \tag{12}$$

As discussed by Jackson [14], the distribution of energy radiated per unit solid angle per unit frequency can be derived by considering the instantaneous radiated power, as described by the Larmor formula, and applying Parsival's theorem. Using the nonlinear electron phase ϕ as the independent variable, we obtain

$$\frac{d^2I(\omega,\mathbf{n})}{d\omega d\Omega}=\frac{e^2\omega^2}{16\pi^3\varepsilon_0 c}\left|\int_{-\infty}^{+\infty}\frac{\mathbf{n}\times[\mathbf{n}\times\mathbf{u}(\phi)]}{\omega_0\gamma_0(1-\beta_0)}\times\exp\left[i\omega\left(\frac{\phi}{\omega_0}+\frac{z(\phi)-\mathbf{n}\cdot\mathbf{x}(\phi)}{c}\right)\right]d\phi\right|^2. \tag{13}$$

The most interesting case is that of the radiation emitted on axis, where most of the power is radiated, and where we obtain the maximum relativistic Doppler upshift. We first consider the forward scattered wave, which is the classical equivalent to stimulated emission, by setting $\mathbf{n}=\hat{\mathbf{z}}$. Equation (13) then reduces to

$$\frac{d^2I(\omega,\hat{\mathbf{z}})}{d\omega d\Omega}=\frac{e^2}{16\pi^3\varepsilon_0 c}\left(\frac{1+\beta_0}{1-\beta_0}\right)\widetilde{\omega}^2\times\left|\int_{-\infty}^{+\infty}\mathbf{a}(\phi)\exp[i\widetilde{\omega}\phi]d\phi\right|^2, \tag{14}$$

where we have introduced the normalized frequency $\widetilde{\omega}=\omega/\omega_0$.

Equation (14) shows that the spectrum of the forward-scattered wave is always similar to that of the laser wave. This is due to the fact that the relativistic Doppler shift on the laser frequency in the electron frame is always exactly compensated by the opposite shift on the forward-scattered radiation. For example, in the case of a linearly polarized Gaussian wave packet of normalized width $\Delta\phi$,

$$\mathbf{a}(\phi)=\hat{\mathbf{x}}a_0\exp\left[-\left(\frac{\phi}{\Delta\phi}\right)^2\right]\exp(-i\phi), \tag{15}$$

the Fourier transform can be evaluated analytically [15] and we find

$$\frac{d^2I(\omega,\hat{\mathbf{z}})}{d\omega d\Omega}=\frac{e^2a_0^2\Delta\phi^2}{16\pi^3\varepsilon_0 c}\left(\frac{1+\beta_0}{1-\beta_0}\right)\widetilde{\omega}^2\exp\left[-\frac{\Delta\phi^2}{2}(\widetilde{\omega}-1)^2\right], \tag{16}$$

which describes a quadratic Gaussian spectrum centered around the normalized frequency $\widetilde{\omega}=1$.

For the backscattered radiation spectrum, we use the result concerning the electron's axial position [Eq. (12)] and recast the expression obtained so that its properties under Lorentz transformation are manifest:

$$\frac{d^2I(\omega,-\hat{\mathbf{z}})}{d\omega d\Omega}=\frac{e^2}{16\pi^3\varepsilon_0 c}\left(\frac{1-\beta_0}{1+\beta_0}\right)\chi^2\left|\int_{-\infty}^{+\infty}\mathbf{a}(\phi)\times\exp\left\{i\chi\left[\phi+\int_{-\infty}^{\phi}\mathbf{a}^2(\psi)d\psi\right]\right\}d\phi\right|^2. \tag{17}$$

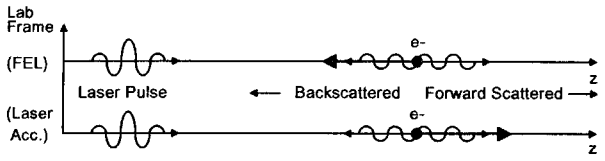

FIG. 1. Geometry of the scattering process.

Here $\chi=(\omega/\omega_0)[(1+\beta_0)/(1-\beta_0)]$ is the normalized Doppler-shifted frequency.

Before studying the nonlinear spectrum, it is interesting to briefly review the case of a Gaussian wave packet [Eq. (15)] of small amplitude, where one can neglect $\mathbf{a}^2$ in the argument of the exponential. Equation (17) can then be integrated analytically [15]:

$$\frac{d^2I(\omega,-\hat{\mathbf{z}})}{d\omega d\Omega}=\frac{e^2a_0^2\Delta\phi^2}{16\pi^3\varepsilon_0 c}\left(\frac{1+\beta_0}{1-\beta_0}\right)\widetilde{\omega}^2\times\exp\left\{-\frac{\Delta\phi^2}{2}\left[\widetilde{\omega}\left(\frac{1+\beta_0}{1-\beta_0}\right)-1\right]^2\right\}. \tag{18}$$

We obtain the usual Doppler-shifted Gaussian radiation spectrum centered around the normalized frequency $\widetilde{\omega}=(1-\beta_0)/(1+\beta_0)$. In the FEL case, $\beta_0\to-1$ and we recover the well-known formula [13] $\widetilde{\omega}\approx4\gamma_0^2$ for an electromagnetic wiggler. We note that the duration of the backscattered pulse is also Doppler compressed, because $\Delta\phi$, which is related to the number of optical oscillations in the pulse, is also a relativistic invariant.

We now focus on the nonlinear effects induced by the variation of the electron Doppler factor along its trajectory. As seen in Eq. (17), the functional dependence of the spectrum is now independent from β_0, which only sets the frequency scale. This fact is not surprising, as it results directly from relativistic invariance: by changing the reference frame in which the scattering process is viewed, one can vary the sign of β_0 and continuously go from the FEL [13] geometry to the laser acceleration [16,17] geometry, both depicted in Fig. 1. For the FEL, the laser frequency is Doppler upshifted in the electron frame, while it is downshifted in the second case. In both cases, the normalized vector potential and the average photon number are conserved as they are Lorentz invariants. In particular, one can choose a frame where the electron is initially at rest.

Having derived the expression for the backscattered light spectrum for an arbitrary polarization state, we will now focus on the two most important cases: circularly and linearly polarized plane waves. The electron dynamics are illustrated in Fig. 2 for both cases.

IV. CIRCULAR POLARIZATION: ANALYTICAL EXPRESSION OF THE FULL NONLINEAR SPECTRUM

We now consider the case of circular polarization, where we have

$$\mathbf{a}(\phi)=g(\phi)[\hat{\mathbf{x}}\sin\phi+\hat{\mathbf{y}}\cos\phi],\quad \mathbf{a}^2(\phi)=g^2(\phi).$$

Here we choose a simple physical model of the pulse envelope, namely, a hyperbolic secant

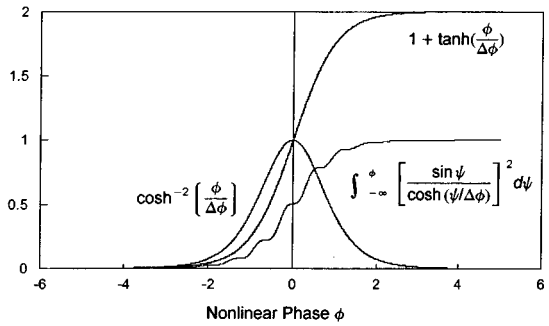

FIG. 2. Behavior of the normalized function $\int_{-\infty}^{\phi}[a^2(\psi)/a_0^2]d\psi$ for circular and linear polarizations.

$$g(\phi)=a_0\cosh^{-1}\left(\frac{\phi}{\Delta\phi}\right). \tag{19}$$

The electron's axial position can then be determined analytically [15] and we have

$$\int_{-\infty}^{\phi}\mathbf{a}^2(\psi)d\psi=\int_{-\infty}^{\phi}\frac{a_0^2 d\psi}{\cosh^2(\psi/\Delta\phi)} =a_0^2\Delta\phi\left[1+\tanh\left(\frac{\phi}{\Delta\phi}\right)\right]. \tag{20}$$

The nonlinear backscattered spectrum is now proportional to

$$\chi^2\left|a_0 e^{i\chi a_0^2\Delta\phi}\int_{-\infty}^{+\infty}\frac{\hat{\mathbf{x}}\sin\phi+\hat{\mathbf{y}}\cos\phi}{\cosh(\phi/\Delta\phi)} \times\exp\left\{i\chi\Delta\phi\left[\frac{\phi}{\Delta\phi}+a_0^2\tanh\left(\frac{\phi}{\Delta\phi}\right)\right]\right\}d\phi\right|^2. \tag{21}$$

To evaluate this Fourier transform, we make a first change of variable and introduce $y=e^{\phi/\Delta\phi}$. The integral in Eq. (21) now reads

$$\Delta\phi\int_0^{+\infty}\frac{y^{i\Delta\phi(\chi\pm1)}}{y^2+1}(\hat{\mathbf{y}}\mp i\hat{\mathbf{x}})\exp\left[ia_0^2\chi\Delta\phi\left(\frac{y^2-1}{y^2+1}\right)\right]dy, \tag{22}$$

where the plus and minus signs simply indicate the different contributions of the sine and cosine functions to the argument of the exponential. We now make a second change of variable, namely, we let $x=(y^2-1)/(y^2+1)$. Equation (22) reduces to

$$\int_{-1}^{+1}(1+x)^{-(1/2)-(i/2)\Delta\phi(\chi\pm1)}(1-x)^{-(1/2)+(i/2)\Delta\phi(\chi\pm1)} \times(\hat{\mathbf{y}}\mp i\hat{\mathbf{x}})\exp[ia_0^2\chi\Delta\phi x]dx, \tag{23}$$

which has an exact analytical expression [15]. The expression for the nonlinear Compton backscattered spectrum can then be given in terms of B, the beta function (Euler's integral of the first kind), and Φ, the degenerate (confluent) hypergeometric function [18]. Using the properties of the beta function and defining $\mu_{\pm}=\frac{1}{2}[1+i\Delta\phi(\chi\pm1)]$, the nonlinear spectrum is shown to further reduce to

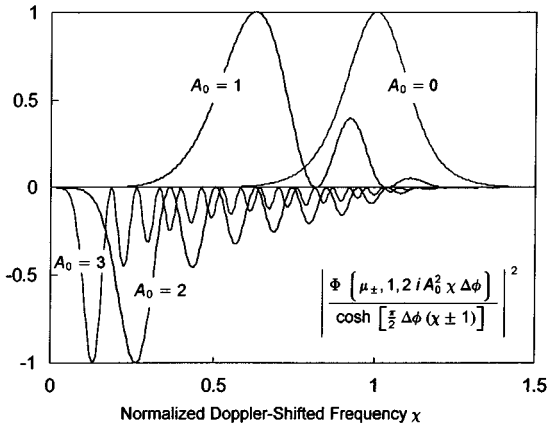

FIG. 3. Behavior of the nonlinear spectral function for circularly polarized light and different values of a_0; $\Delta\phi=5$.

$$\frac{d^2I(\omega,-\hat{\mathbf{z}})}{d\omega d\Omega}=\frac{e^2a_0^2\Delta\phi^2}{8\pi\varepsilon_0 c}\left(\frac{1-\beta_0}{1+\beta_0}\right) \times\chi^2\left\{\left|\frac{\Phi(\mu_-,1,2ia_0^2\chi\Delta\phi)}{\cosh\left[\frac{\pi}{2}\Delta\phi(\chi-1)\right]}\right|^2 +\left|\frac{\Phi(\mu_+,1,2ia_0^2\chi\Delta\phi)}{\cosh\left[\frac{\pi}{2}\Delta\phi(\chi+1)\right]}\right|^2\right\}. \tag{24}$$

At low intensity ($a_0\ll1$), $\Phi\sim1$ and we recover the Doppler-shifted $\cosh^{-2}$ spectral line.

To understand the physics of this solution at high intensities, it is useful to expand Φ into a Bessel function series [18]

$$\Phi(\mu,1,z)=e^{z/2}\Gamma(\tfrac{1}{2}-\mu)\left(\frac{z}{4}\right)^{\mu-1/2}\sum_{n=0}^{\infty}\left[\frac{(1-2\mu)_n}{n!}\right]^2 \times(n+\tfrac{1}{2}-\mu)(-1)^nI_{n+1/2-\mu}\left(\frac{z}{2}\right), \tag{25}$$

where $z=2ia_0^2\chi\Delta\phi$ and the notation $(c)_n$ is defined as $(c)_n=c(c+1)\cdots(c+n-1)$.

The behavior of the nonlinear spectral function $|\Phi(\mu,1,2ia_0^2\chi\Delta\phi)/\cosh[(\pi/2)\Delta\phi(\chi-1)]|^2$ is illustrated in Fig. 3 for $\Delta\phi=5$ and different values of a_0. As a_0 augments past unity, the imaginary argument increases quadratically and higher-order Bessel functions are excited, corresponding to an increasing number of spectral lines. Within this context, the onset of nonlinear relativistic spectral effects corresponds to a situation where ϕ and $\int_{-\infty}^{\phi}\mathbf{a}^2(\psi)d\psi$ become comparable.

Although the derivation presented here is purely classical, it is interesting to translate Eq. (24) into an average number of photon radiated per unit frequency per unit solid angle by dividing this equation by $\hbar\omega$. The resulting nonlinear spectral and angular distribution of the photon probability density is presented in Fig. 4 and the spectral lines can now be tentatively identified with nonlinear $1,2,\ldots,n$ photon pro-

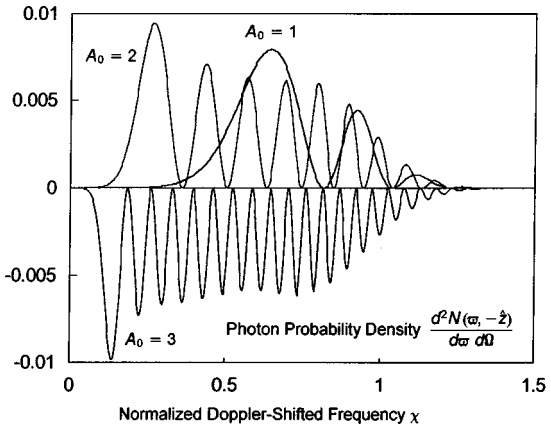

FIG. 4. Backscattered photon probability density per unit solid per unit frequency in the case of a circularly polarized hyperbolic secant pulse of width $\Delta\phi=5$, for different intensities.

cesses. In that case, the effect of a multiphoton interaction can be described as a combination of ponderomotive recoil and harmonic generation.

The most important consequence of the nonlinear Doppler effect, however, resides in the fact that, at ultrahigh intensities, the peak photon number density in each line is approximately constant across the spectrum. This indicates that for ultrashort laser pulses, even in the case of circularly polarized light, the backscattered energy is redistributed over a wide spectral range instead of contributing to a single, narrow Compton backscattered line. This is a potentially serious difficulty for applications, such as the γ-γ collider, which require the generation of a single, intense, highly collimated, narrow γ-ray line. Such a problem can be partially alleviated by shaping the temporal envelope of the pump laser pulse in order to minimize the nonlinear Doppler shift during the interaction. In such a scheme, as illustrated in Fig. 5 (top), the main part of the laser pulse is flat, thereby yielding constant axial electron velocity during most of the interaction. The associated Doppler shift thus remains nearly constant, resulting in the radiation of a narrow spectral line, as indicated in Fig. 5 (bottom). During the rise and fall of the laser pulse envelope, transient lines are radiated, but they are kept to a minimum by using this technique, which is rather analogous to the use of a tapered wiggler entrance for a FEL [13].

This procedure can be modeled theoretically by considering a circularly polarized pulse with a composite envelope, including a hyperbolic secant rise and fall and a constant flat top:

$$g(\phi)=a_0\cosh^{-1}\left(\frac{\phi}{\Delta\phi}\right), \quad \phi\leqslant 0 \tag{26a}$$

$$g(\phi)=a_0, \quad 0\leqslant\frac{\phi}{\Delta\phi}\leqslant\eta \tag{26b}$$

$$g(\phi)=a_0\cosh^{-1}\left(\frac{\phi}{\Delta\phi}-\eta\right), \quad \frac{\phi}{\Delta\phi}\geqslant\eta. \tag{26c}$$

The resulting axial electron position is now given by

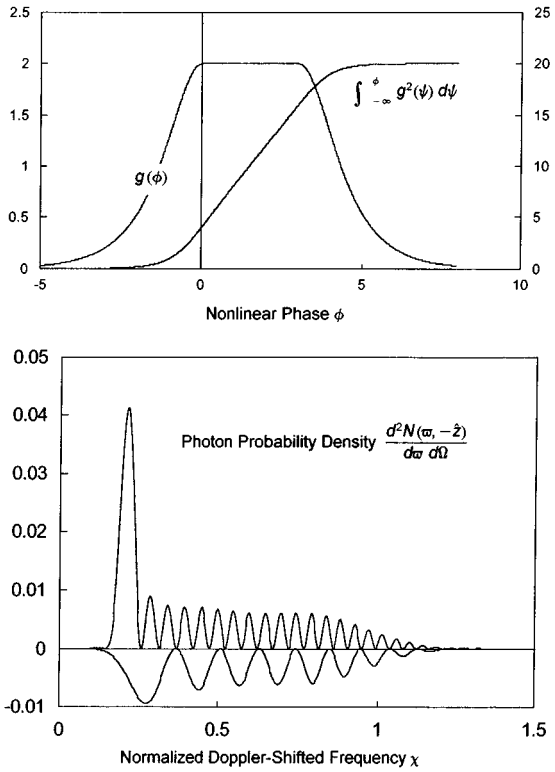

FIG. 5. Top: hyperbolic secant pulse envelope with a flat top ($\Delta\phi=5$, $a_0=2$, and $\eta=3$) and normalized axial position. Bottom: comparison of the backscattered photon probability density for the same pulse with and without a flat top.

$$\int_{-\infty}^{\phi}\mathbf{a}^2(\psi)d\psi=a_0^2\Delta\phi\left[1+\tanh\left(\frac{\phi}{\Delta\phi}\right)\right], \quad \phi\leqslant 0 \tag{27a}$$

$$\int_{-\infty}^{\phi}\mathbf{a}^2(\psi)d\psi=a_0^2(\Delta\phi+\phi), \quad 0\leqslant\frac{\phi}{\Delta\phi}\leqslant\eta \tag{27b}$$

$$\int_{-\infty}^{\phi}\mathbf{a}^2(\psi)d\psi=a_0^2\Delta\phi\left[1+\tanh\left(\frac{\phi}{\Delta\phi}-\eta\right)+\eta\right], \quad \frac{\phi}{\Delta\phi}\geqslant\eta. \tag{27c}$$

It is easily seen that in the nonlinear Fourier integral [Eq. (17)], Eqs. (27a) and (27c) can be grouped together, as they differ only by a constant phase shift. The corresponding integral is then directly obtained by the changes of variables described in Eqs. (21)–(23). The contribution of the flat top is simply proportional to

$$a_0 e^{i\chi a_0^2\Delta\phi}\int_0^{\eta\Delta\phi}(\hat{\mathbf{x}}\sin\phi+\hat{\mathbf{y}}\cos\phi)\exp[i\chi\phi(1+a_0^2)]d\phi, \tag{28}$$

where we recognize the factor $1+a_0^2$, which lowers the relativistic Doppler shift. The integral in Eq. (28) is readily performed to yield a sinc spectrum.

It is clear that for $\eta\gg 1$, the line at the normalized Doppler-shifted frequency $\chi=1/(1+a_0^2)$ dominates the backscattered spectrum, as shown in Fig. 6 ($\eta=10$). The shorter wavelength lines correspond to a combination of the multiphoton lines resulting from the nonlinear Doppler shift dur-

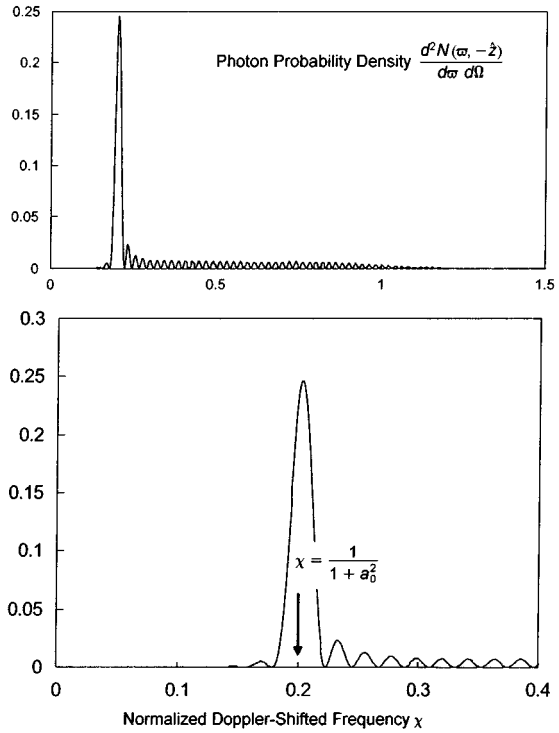

FIG. 6. Backscattered photon probability density for a longer flat top (η=10) pulse; the other parameters are the same as in Fig. 5. The bottom figure shows a closeup of the main spectral line.

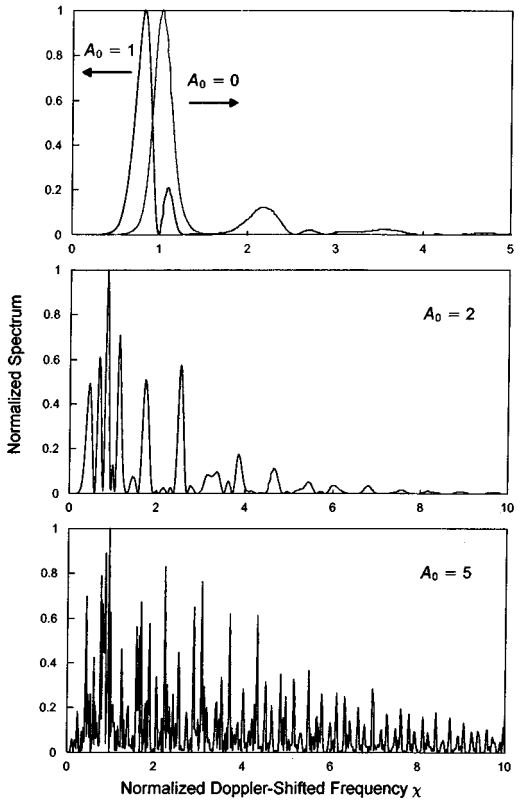

FIG. 7. Normalized backscattered radiation spectra for a linearly polarized hyperbolic secant pulse of width $\Delta\phi$=5 and increasing laser intensities.

ing the transient parts of the pulse and the oscillations of the sinc spectrum associated with the rectangle window in Eq. (28). The relatively long flat top both enhances the contrast between the nonlinear transient lines and the main line and narrows the spectral width of the radiation backscattered at maximum laser intensity (constant Doppler shift).

V. LINEAR POLARIZATION

In the case of linear polarization, no simple analytical derivation of the full nonlinear spectrum has been obtained yet. This is due in part to the extra modulation of the electron axial momentum at the second harmonic of the laser Doppler-shifted frequency. Therefore, in this section, we study the interaction of linearly polarized laser pulses with a relativistic electron by performing the Fourier transform in Eq. (17) numerically.

Figure 7 illustrates the evolution of the normalized backscattered radiation spectrum with the laser intensity, in the case of linear polarization. For a_0=0, one obtains the expected linear FEL Doppler-shifted $\cosh^{-2}$ spectrum at χ=1. For a_0=1, the main spectral line is shifted from the normalized value of 1, because the average electron velocity differs from β_0 during the interaction; some additional nonlinear spectral features start to appear. At higher laser intensities, the onset of relativistic anharmonicity is clearly visible. In particular, the amplitude of the main spectral lines does not increase as a_0^2; instead, the energy is redistributed over a ''dense'' spectrum, thus indicating the excitation of new oscillation modes [19], each corresponding to a degree of freedom. A parametric study indicates that these results depend only weakly on $\Delta\phi$.

The main difference between polarization states resides in the fact that at high intensities, the extra modulation term at $2\omega_0$ (see Fig. 2), which characterizes linearly polarized light, yields arbitrarily short-wavelength lines, while the nonlinear spectrum for circular polarization appears to be bounded to subharmonics of the Doppler-shifted laser line (Fig. 4). In both cases, however, the full nonlinear Compton backscattered spectra become very complex at high field strengths.

These results are relevant to the nonlinear Compton scattering experiments currently underway at SLAC [12], as well as to the proposed γ-γ collider: for such experiments, the nonlinear Doppler shift is a first-order effect, even for circularly polarized light, and dominates over the recoil effect (electron self-interaction) associated with nonlinear Compton scattering.

It is quite remarkable that such an elementary electrodynamical process as the scattering of coherent light by a single electron describing a well-behaved trajectory can yield relativistic spectral effects when the laser ponderomotive force strongly modulates the electron's proper time. This suggests that, in this case, nonlinear spectral features arise from the local variation of the relativistic Doppler shift. In other words, as clocks in the laboratory frame and in the electron's instantaneous rest frame cannot be synchronized, the coherent light signal scattered by the electron appears anharmonic to any observer in uniform motion with respect to the laboratory frame.

VI. CONCLUSION

The relativistic dynamics of an electron subjected to the classical electromagnetic field of an ultrashort laser pulse has

been studied theoretically at arbitrary intensities. Frequency modulation effects associated with the nonlinear relativistic Doppler shift induced on the backscattered radiation were investigated in detail. For circular polarization, an exact analytical expression for the full nonlinear spectrum has been derived. For linear polarization, it was found that the scattering of coherent light by a single electron describing a well-behaved trajectory can yield anharmonic spectra when the laser ponderomotive force strongly modulates the electron's proper time. These nonlinear relativistic spectra exhibit complex structures. It is quite remarkable that such an elementary electrodynamical process can yield relativistic spectral effects when the laser ponderomotive force strongly modulates the electron's proper time. This suggests that, in this case, nonlinear spectral features arise from the local variation of the relativistic Doppler shift.

In addition, it was shown that circularly polarized laser pulses with a flat top are best suited to generate narrow Compton backscattered spectral lines at ultrahigh intensities. In this case, the relatively long flat top both enhances the contrast between the nonlinear transient lines and the main line and narrows the spectral width of the radiation backscattered at maximum laser intensity (constant Doppler shift). Experimental studies of these phenomena, using a 50-TW CPA laser and a mildly relativistic electron beam, are planned to be performed in the near future, and the implementation of holographic filtering [11] on a CPA laser to obtain flat-top pulses are planned to be presented in an upcoming paper.

ACKNOWLEDGMENTS

This work is supported in part by the AFOSR (ATRI) under Grant No. F30602-94-2-0001, in part by ARO under Grant No. DAAHO4-93-0084, and in part by LLNL/LDRD Contract No. W-7405-ENG-48. We wish to acknowledge very stimulating discussions with J. G. Woodworth, M. D. Perry, Professor A. K. Kerman, Professor J. P. Heritage, and E. D. Parayo.

[1] L. F. Mollenauer, R. H. Stolen, and J. P. Gordon, Phys. Rev. Lett. **45**, 1095 (1980).
[2] H. A. Haus, J. G. Fujimoto, and E. P. Ippen, IEEE J. Quantum Electron. **QE-28**, 2086 (1992).
[3] P. Maine, D. Strickland, P. Bado, H. Pessot, and G. Mourou, IEEE J. Quantum Electron. **QE-24**, 398 (1988).
[4] F. G. Patterson and M. D. Perry, J. Opt. Soc. Am. B **8**, 2384 (1991).
[5] M. D. Perry and G. Mourou, Science **264**, 917 (1994).
[6] F. V. Hartemann *et al.*, Phys. Rev. E **51**, 4833 (1995).
[7] F. V. Hartemann and N. C. Luhmann, Jr., Phys. Rev. Lett. **74**, 1107 (1995).
[8] H. A. Haus, Am. J. Phys. **54**, 1126 (1986).
[9] P. A. M. Dirac, Proc. R. Soc. London Ser. A **167**, 148 (1938).
[10] F. V. Hartemann and A. K. Kerman, Phys. Rev. Lett. **76**, 624 (1996).
[11] B. H. Kolner, IEEE J. Quantum Electron. **QE-30**, 1951 (1994).
[12] C. Bula *et al.* (unpublished).
[13] C. W. Roberson and P. Sprangle, Phys. Fluids B **1**, 3 (1989).
[14] J. D. Jackson, *Classical Electrodynamics*, 2nd ed. (Wiley, New York, 1975), Chaps. 14 and 17.
[15] I. S. Gradshteyn and I. M. Ryzhik, *Table of Integrals, Series and Products* (Academic, Orlando, 1980).
[16] C. E. Clayton, K. A. Marsh, A. Dyson, M. Everett, A. Lal, W. P. Leemans, R. Williams, and C. Joshi, Phys. Rev. Lett. **70**, 36 (1993).
[17] M. S. Hussein, M. P. Pato, and A. K. Kerman, Phys. Rev. A **46**, 3562 (1992).
[18] *Handbook of Mathematical Functions*, edited by M. Abramowitz and I. A. Stegun (Dover, New York, 1972).
[19] D. Rand, S. Ostlund, J. Sethna, and E. D. Siggia, Phys. Rev. Lett. **49**, 132 (1982).